INTERNATIONAL JOURNAL FOR NUMERICAL METHODS IN FLUIDS, VOL. 8, 1491–1511 (1988)

THE ANALYSIS OF GLASS MELTING PROCESSES USING THREE-DIMENSIONAL FINITE ELEMENTS

R. A. MURNANE, W. W. JOHNSON AND N. J. MORELAND

Thermal Process Engineering and Development, Melting Technology, Corning Glass Works, Corning, New York 14831, U.S.A.

SUMMARY

Traditionally glass process problems have been studied using laboratory and two-dimensional computer simulation techniques to quantify the melting, cooling and distribution of the molten glass and its quality. Although these approaches are adequate for a large number of simple glass systems, there are processes with asymmetric geometries and operating conditions which cannot neglect the effect of the third dimension. During the past few years, with the advent of commercial parallel processors and corresponding software, extensive progress has been made with the implementation of full three-dimensional glass flow simulations. Several development applications using FIDAP will be illustrated for electric melters, circular refiners and contoured forehearths. The discussion will cover the problem set-ups, mesh generation, solution strategy, post-processing and results. The advantages and developmental needs of FIDAP will be highlighted from the point of view of applied glass process engineering.

KEY WORDS Glass process engineering Melting 3D finite elements FIDAP

INTRODUCTION

Development of modelling simulations for hot glass processes has been a continuing project in Corning Glass Works and the glass industry since the early 1940s. Methods using the entire range of modelling tools have been designed to duplicate the momentum, heat and mass transport phenomena in melters, refiners, distributors and forehearths. These approaches include full-scale oil modelling of channel stirring, bench-scale physical modelling of all-electric melting, laboratory modelling of fusion kinetics and computer modelling of free-convective circulations.[1–5]

Through the late 1970s, the analyses of glass flow and heat transfer problems had been approached using two-dimensional (2D) mathematical models with assistance from laboratory simulations to describe the effect of the third dimension. The computer software and hardware for full three-dimensional (3D) studies were costly and cumbersome to implement.

The dual technique of applying 2D mathematical and 3D physical models has proven to be an effective tool because it provides a quick, economical testing of various process designs.[6] In conjunction with a systems engineering approach which incorporates knowledge of the glass chemistry along with the momentum and heat transfer phenomena, these methods can be extremely useful in determining the best design or operational solution to the problem.[7] They remain the standard engineering approach taken in the vast majority of melting process problems.

In the early 1980s, with the advent of commercial high-speed computers and compatible software which took advantage of parallel processing, the potential to use 3D computer models for glass process analysis was established. During this time, process engineers within Corning Glass

0271–2091/88/121491–21$10.50

Received 25 November 1987
Revised 25February 1988

Works (CGW) were attempting to apply production optimization methods to all the hot glass lines. Much information about the dynamics of some systems was found not to exist because the inherent complexity of the 3D geometry and operations had been ignored or overly simplified. Past analyses characterized the systems in relation to symmetric boundary conditions and approximated the geometries using 2D rectangular or cylindrical sections. As the attempt to understand the processes increased, these assumptions were found to be inadequate when applied to systems with operational asymmetries (e.g. all-electric melting with batch electrodes, refiners with multiple forehearths) and with complex geometries or cooling distributions (e.g. distributor to multiple channels, forehearth channels, bowls).

To determine the benefits of the 3D computer applications, CGW established a program to implement this technique on production problems which had heretofore been neglected. The objective was to use the 3D tool to gain a deeper insight into the controlling process parameters to give guidance to changes in operational set-ups or in proposed design changes. When applied by an experienced process analysis engineer, the computer program had to

(1) detail the interaction of the heat transfer and glass flow under both steady state and transient conditions
(2) represent complex geometries
(3) test limiting operating conditions by using parametric analyses
(4) be cost effective enough to reduce the amount of in-plant experimentation and to evaluate the implications of process design changes.

Using available commercial software programs has several advantages. They eliminate the development costs associated with writing a program in-house, minimize the need for engineering experience in numerical programming, supply state-of-the-art computer graphics for pre- and post-processing of the data, and provide vendor services such as technical consultation and regular program revisions.

The Fluid Dynamics International's (FDI) FIDAP finite element software has been used in many types of CGW production situations. This paper uses several examples to highlight the advantages and developmental needs of FIDAP from the point of view of applied glass process engineering.

MODELLING APPLICATIONS

CGW's process analysis engineers encounter a wide variety of glass process problems. Several examples will be given showing the application of the FIDAP program for process development of new technology (operation of an all-electric melter), for process design changes (modification of a television panel glass refiner) and for process problem solving (forehearth and bowl well flow study). Each case will discuss the probelm set-up, mesh generation, solution strategy, post-processing and results.

PROCESS DEVELOPMENT—SUMMIT™MELTER

CGW has developed a new generation of all-electric, molybdenum-lined glass melting systems. The conceptual design of these Summit™ melters was based on an extensive modelling program, including 2D mathematical modelling, small-scale physical modelling and laboratory melting simulations. Based on the concepts recommended from these studies, Summit™ furnaces have been built and operated to meet widely varying process requirements ranging from 10 to 50

tons/day at temperatures of 1450–1800 °C. Figure 1 shows an illustration of the interior of a Summit™ melter.

High thermal efficiency and long tank life are the major benefits of the Summit™ melter. A molybdenum liner containing the hot glass is designed to protect the refractory from corrosion. This allows the use of a high degree of insulation on the refractory structure.

The unit is operated with a continuous batch of the solid raw materials fed on top of the melter through a rotating chute. The thick batch crust floats on top of the molten glass surface, acting as a thermal insulator and capturing polluting or volatile chemicals. The glass is withdrawn through a horizontal molybdenum pipe with the entrance centred on the bottom and passing through a side wall into the delivery system.

Energy to melt the batch is supplied by batch electrodes—molybdenum rods inserted at various radial and angular positions through the batch floating on the molten glass. The localized hot spots near the electrodes, the energy sink at the batch/molten glass interface and the heat losses

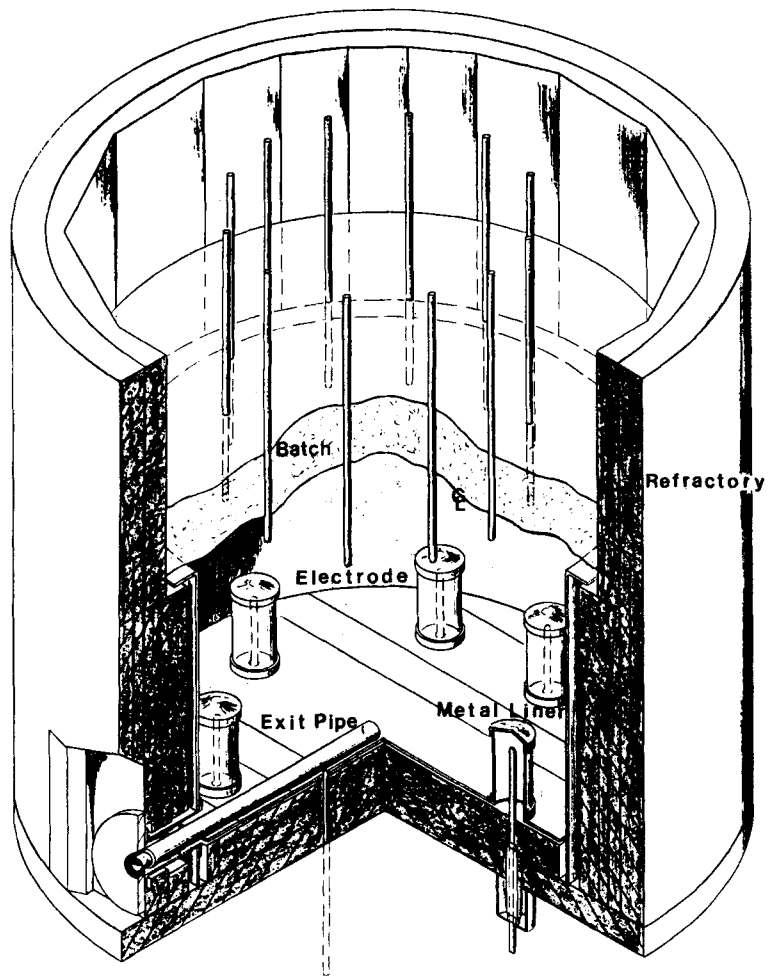

Figure 1. Summit™ melter physical design

through the tank walls create thermally induced free convective currents in the melter. Understanding this fluid motion is important for designing such units.

Producing a defect-free glass product requires exposing the glass to an adequate time–temperature history such that silica grains go into solution and gaseous bubbles are absorbed or removed through the batch layer. The residence times and temperature fields in the melter are critical to the batch melting and gas bubble removal processes. Mathematical modelling allows us to study these important parameters.

Production melter tracer studies have not agreed well with minimum residence times (MRT) from the 2D and physical models. Also, the models could not predict the changes that resulted from moving the batch electrodes to new positions.

Owing to the inability of the 2D model to account for the angular placement of electrodes and the deficiency of the physical model to meet exact process similarity conditions, a 3D mathematical model was developed to investigate the impact of electrode position on residence time.

Melter mathematical model and numerical method

The problem used standard assumptions for the analysis of glass processes. The mathematical model used the steady-state incompressible Newtonian fluid equations with the Boussinesq assumption to account for density variation. The boundary conditions for the Summit™ problem were a combination of velocity profiles and heat transfer coefficients. These specifications described the effects of the melting interface along the top boundary and the heat losses through the different refractory materials along the liner wall and the melter bottom. The momentum boundary conditions had zero-velocities at the bottom and liner, symmetry planes and centreline, a specified inlet velocity profile along the top of the melter and a free boundary at the outlet pipe. The thermal boundary conditions used heat transfer coefficients along the liner and bottom and source terms at the melting interface and electrode positions. The incompressibility constraint and the pressure variable were accounted for by using the penalty approach.

The development of a mesh utilizing brick elements which provided adequate resolution of the solution, a reasonable matrix size and balanced element aspect ratios was challenging. 2D tests were used to determine a suitable grid pattern before attempting a 3D case. Initial simulations showed oscillations in the velocity vectors, indicating that dense nodal refinement was needed at the side and bottom walls and especially around the exit pipe. The region near an electrode needed refinement not only due to the high convective velocities at this hot spot but also due to the high concentration of electric power.

With a rectangular grid, FIMESH lines are propagated through both logical space and the solution domain. Regions not needing a dense mesh have an unnecessary number of nodes. Meshes which contained 10000 nodal points were needed in order to get the necessary mesh density near the walls with element aspect ratios small enough to resolve the large gradients there. This made it uneconomical to conduct a full series of parametric variations.

To resolve this problem, a mesh was generated using PDA/PATRAN-G, a dedicated pre- and post-processor. The construction of the mesh took advantage of the topological zoom feature, which allowed the necessary local mesh refinement. Wedge-shaped elements were used on the centreline to easily conform to the problem geometry. A program supplied by FDI converted the PATRAN neutral file output to a FIPREP/FIMESH compatible file.

No additional mesh refinement was made after the problem size was reduced and the oscillating velocity vectors eliminated. Figure 2 shows the final mesh which characterized these critical regions. An initial 15° wedge was chosen spanning from one electrode to the centre plane between electrodes.

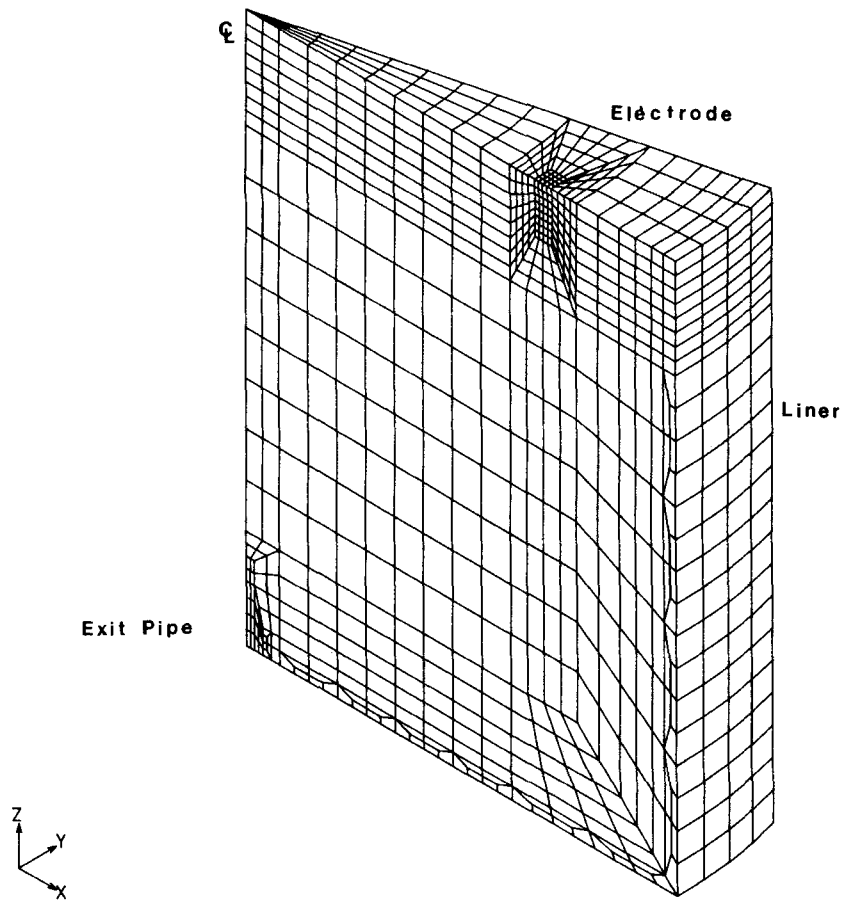

Figure 2. Summit™ mesh geometry—electrode plane

The electrodes inserted through the batch layer generate a power field using alternating current resistive heating. Figure 3 shows the typical power distribution using lines of constant power density. The field is concentrated near the electrodes and decreases rapidly with distance from the electrode. This creates thermal hot spots in the melter positioned at the electrodes which become the main driving force for the free convection cells.

FIDAP had to simulate the power dissipation field generated by these batch electrodes. Assuming that the electrical resistivity of the glass is independent of temperature, the power field can be calculated apart from the temperature and flow fields. A separate CGW program was used to calculate the voltage field and the subsequent power dissipation field by a finite difference method. Twelve electrodes were arranged in a ring, spaced 30° apart. Opposing electrodes (out of phase electrically by 180°) comprised a circuit. A unit voltage field was calculated for each circuit by solving the three-dimensional Laplace equation governing the voltage distribution in an electrical field. Special boundary conditions such as the zero potential on the molybdenum liner and the zero voltage gradient normal to the batch layer and the bottom refractory were included. A root-mean-square voltage field was claculated by the superposition of the unit voltage fields using the phase angles and powers on each circuit. Power dissipation was calculated by integrating the product of voltage and current density over an element's surface.

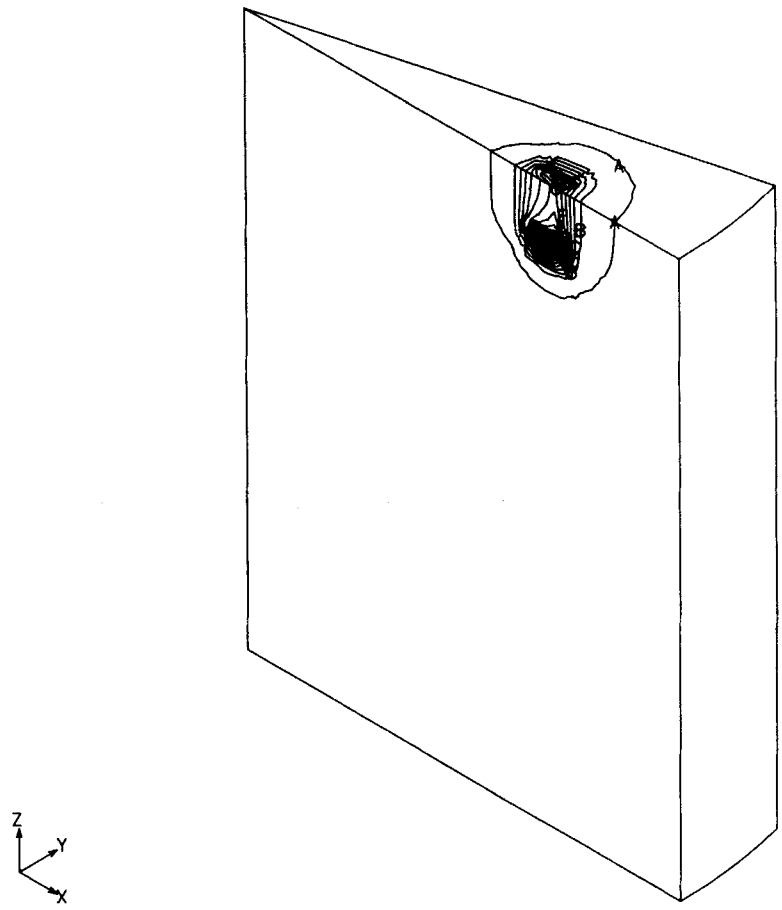

Figure 3. Summit™ melter power density contours

To put the power density data into a useful form for FIDAP, these results were interpolated from the finite difference grid to the finite element mesh and inserted into an output file. This file was initially read in the energy source term subroutine HSORCE and stored in a variable array for subsequent calls. Additional FORTRAN statements were added to subroutines FLW3D and FORCL3 to calculate the total power dissipated by integrating over all the element volumes. An overall energy balance was made to check the routine.

Melter results and discussion

The molten glass in a melter is characterized by high Grashof, high Prandtl and low Reynolds numbers; Table I summarizes the values of these dimensionless numbers for the Summit™ process. With the strong circulating free convective flows caused by the temperature gradients dominating the forced convection due to the hydrostatic forces, FIDAP was used to slowly add the influence of the buoyancy term in order to obtain a converged solution.

The strategy used was to approach the full effect of the volumetric expansion coefficient independent of the effects due to forced convection and non-linear temperature-dependent viscosity and thermal conductivity by gradually increasing the expansion coefficient from one run

Table I. Summit™ melter dimensionless numbers

Reynolds (1300 °C)	$1{\cdot}89 \times 10^{-3}$
Prandtl (1300 °C)	582
Grashof (1300 °C)	314
Nusselt (Top, average)	1·2
Nusselt (Side, average)	0·025
Nusselt (Bottom average)	0·125

Table II. Summit™ melter problem size

Number of nodes	3026
Number of 3D elements	2336
Number of equations	9917
Number of matrix elements	10162705
Mean 1/2 bandwidth	512
Maximum 1/2 bandwidth	739

Table III. Summit™ computation time on FPS 264

BETA/1000	3 Newton–Raphson	54 min
BETA/100	4 NR	72 min
BETA/10	10 NR 0·5 acceleration factor	180 min
BETA	10 NR 0·5 ACCF	180 min
Forced convection flow	5 NR 0·5 ACCF	90 min
Temperature-dependent thermal conductivity	5 NR 0·5 ACCF	90 min
Temperature-dependent viscosity	5 NR 0·5 ACCF	90 min
Total		756 min

to the next. This technique will be referred to as using 'loading' steps. For the initial case the expansion coefficient was set to several orders of magnitude below its final value and was increased by a factor of 10 for each loading step. The forced convection flow was suppressed and constant physical properties were used. The Newton–Raphson method converged to within 0.1% relative error in the velocity with three to ten iterations, depending on the value of the loading parameter. An acceleration factor of 0.5 improved the robustness of the method at the higher loading steps.

The machine used for the computations is a Floating Point System (FPS) 264 array processor using the fast matrix solver (FMS) library. Table II contains information about the problem size for a typical Summit™ case. Table III shows the elapsed time on the FPS 264 for solving the problem using a VAX 780 as the host device. The I/O operations with this system were the largest time factor. Approximately 4 min of the total 18 min for an iteration was used for computation.

Post-processing was performed using the FIPOST program in FIDAP. Results are shown in Figures 4 and 5 using velocity vectors; a horizontal plane cut just below the top inlet plane is used

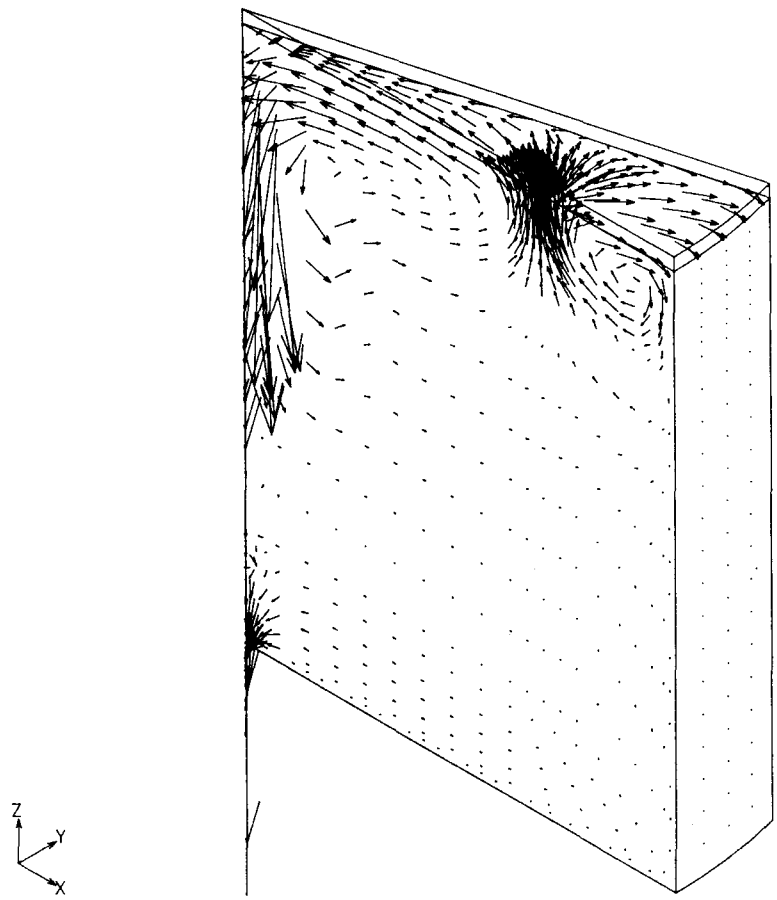

Figure 4. Summit™ melter velocities—electrode plane

to follow the glass movement near the electrode. The hot spot at the electrode generates an ascending flow which descends at the wall and at the centre of the melter. High velocities occur near the inner radius as glass converges towards the centreline. There is a tendency for glass to flow from the electrode toward a position near the wall between electrodes. This phenomenon creates two convective rolls in the upper region of the tank. The high velocities produced by the batch electrodes cause rapid melting and mixing.

Generally vertical melters are characterized by an active upper region and a quiescent lower zone. In a Summit™ the flow down the walls is much slower than in a refractory vertical melter since the walls are well insulated. The greatly reduced cross-sectional flow area near the exit pipe produces the highest velocities in the unit.

Figures 6 and 7 are plots of temperature contours. Convection has a large influence on the temperature distribution in the glass bath. The highest concentration of power occurs at the tip of the electrode, but convection has raised the position of the maximum temperature to a region on the electrode above the tip. The distortion in the isotherms in the upper region of the melter due to convection is evident. In the lower regions of the melter the reduced velocities allow thermal conduction to dominate as shown by the parallel isotherms.

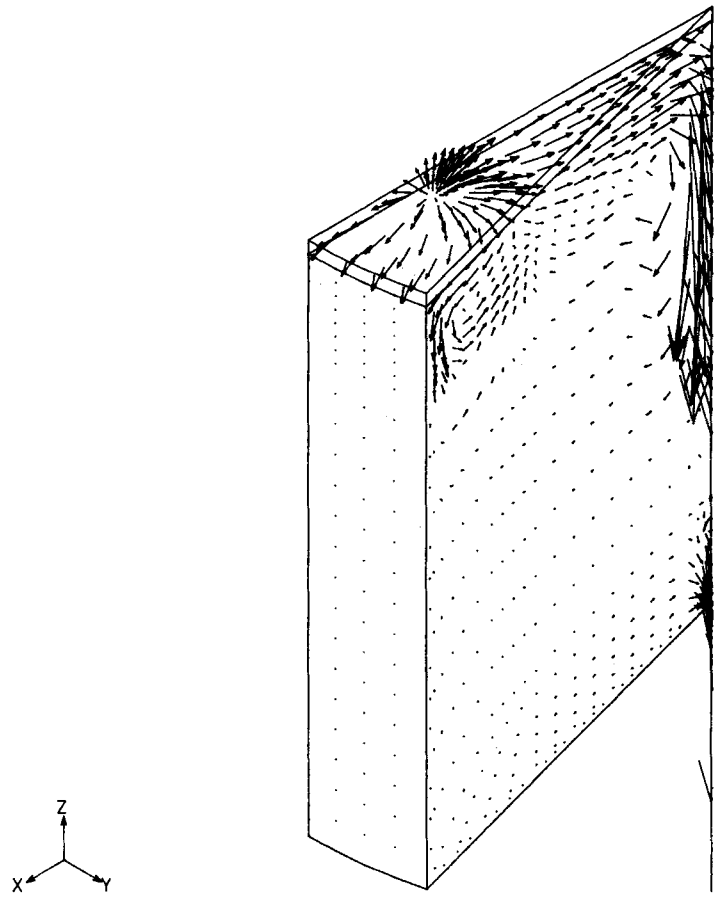

Figure 5. Summit™ melter velocities—intermediate plane

PROCESS DESIGN CHANGES—TELEVISION REFINER

A new furnace has been designed for a television panel glass. The proposed circular distribution chamber's (refiner) radius for the new tank was increased to accommodate the higher flow rates expected in the new furnace. Concerns were raised over what effect the radius and flow changes would have on the temperature homogeneity of the glass at the entrance into the refractory channels used to cool the glass (forehearths). Any areas of stagnation would also pose a problem since they would be considered as potential sources affecting glass quality.

During the study of several refiner concepts for this design change, some general solution strategies for high-Rayleigh-number, low-Reynolds-number models were developed. These strategies will be illustrated using results from one concept of the television refiner.

The function of a refiner is to distribute the molten glass from the melting furnace to the forehearths, cooling the glass so that it is at the correct temperature at the forehearth entrance. Figure 8 shows a cut-out illustration of the main refractory components of a refiner enclosing the glass and the combustion chamber above the glass surface. The expected flow pattern is one

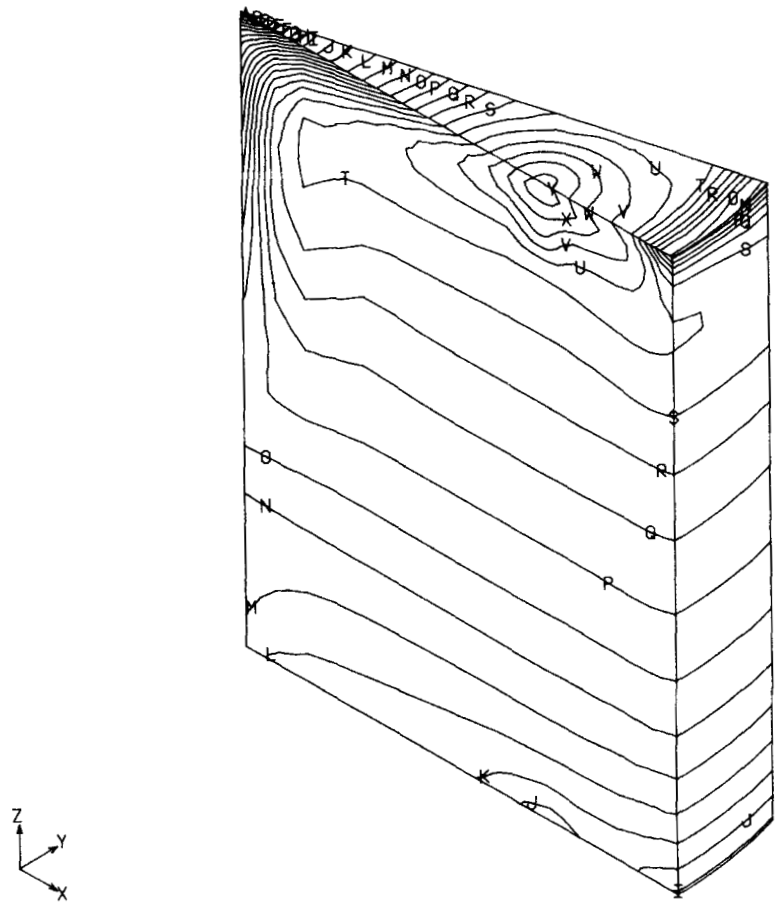

Figure 6. Summit™ temperature contours—electrode plane

convective roll moving the glass from the throat entrance up to the glass surface, across the cooling surface to the walls, down the walls and back toward the throat along the bottom.

Television refiner mathematical model and numerical method

The overall strategy for this type of problem was similar to that used in the Summit™ case—to 'step up' the flow conditions from a low Rayleigh value to the final level by one order of magnitude increase each step using the characteristic momentum and heat transfer equations for an incompressible Newtonian fluid with the Boussinesq assumption and the penalty method.

The refiner that was modelled is circular, but only half of the refiner geometry was used by assuming a plane of symmetry down the vertical centreline plane. Figure 9 shows the mesh of the refiner using brick elements. The model includes one forehearth connection, one half of the overflow located on the nose and one half of the tap located in the centre bottom of the refiner.

The glass inlet temperature and velocity at the throat were specified, as well as flow rates on the forehearth, overflow and tap. Heat transfer coefficients for refractory conduction and air temperatures above the glass surface for radiation were used to account for the energy losses.

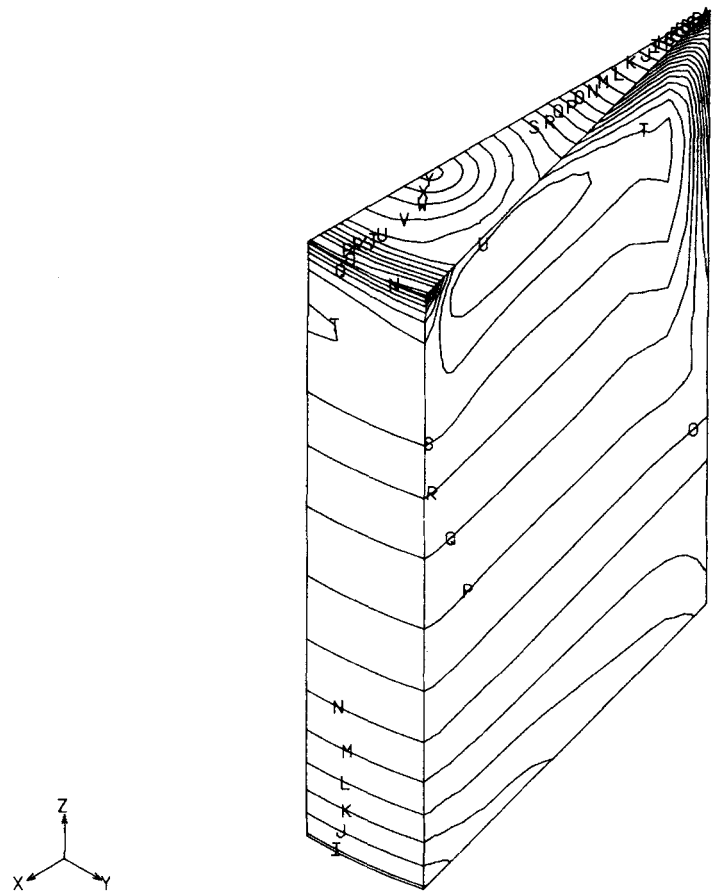

Figure 7. Summit™ temperature contours—intermediate plane

Table IV. Television refiner problem size

Number of nodes	3856
Number of 3D elements	3160
Number of equations	12436
Number of matrix elements	15478162
Mean 1/2 bandwidth	622
Maximum 1/2 bandwidth	1227

Television refiner results and discussion

The machine used for the computations was the same FPS 264 array processor used for the Summit™ problem. Table IV contains information about the problem size for a typical refiner case. The average solution time per loading step was of the order of 25 min.

For the refiner model with a Rayleigh number of the order of 10^6, a typical set of runs would begin with the isothermal solution and proceed through the non-isothermal cases starting with a

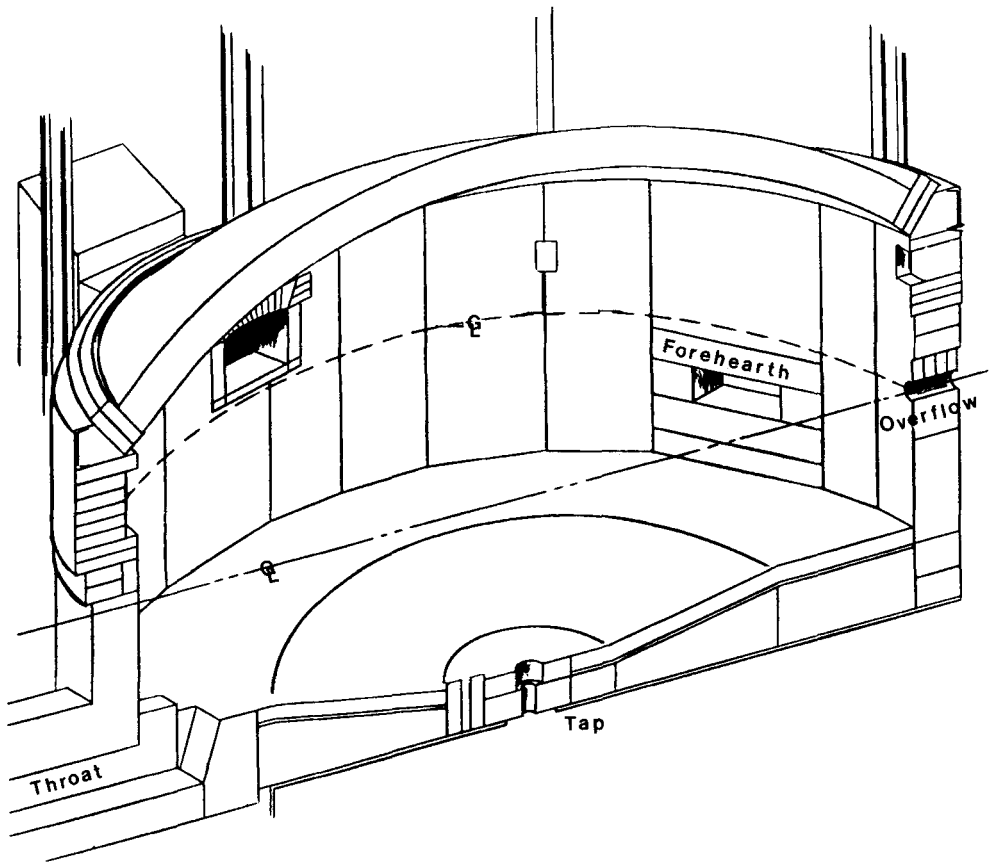

Figure 8. Television refiner physical design

Rayleigh value of 10^3. The usual scheme is to start each loading step with one to three successive substitution (SS) iterations followed by several Newton–Raphson (NR) iterations. For Rayleigh values up to 10^4 the solution for the glass refiner model converged easily with this strategy. The flow pattern for the converged run of Rayleigh number equal to 10^4 is shown in Figure 10.

When stepping to a Rayleigh number of 10^5 the solution would not converge, but neither would it diverge. The values of FIDAP's two convergence criteria, 'Rel error of velocity' and 'Rel error of F', did not change much between any of the iterations. Figures 11 and 12 show the flow patterns after three and six SS iterations respectively. All of the flow patterns seem to be 'wandering' from the expected pattern shown in Figure 10.

It was discovered that SS interations could not be used at the higher Rayleigh values. Any time that SS iterations were specified, the 'wandering' flow pattern was seen. If only NR iterations are used, the problem converges easily. The strategy of using SS iterations only on the initial series of loading steps and then using NR iterations for the final steps has worked well.

This procedure has become the standard approach for all later studies of flows with strong circulating flows. For some situations an acceleration may be necessary. If an order-of-magnitude step in Rayleigh number causes divergence, it is recommended to include the FIDAP numerical acceleration factor, ACCF, with a value from 0.25–0.5 in the solution strategy.

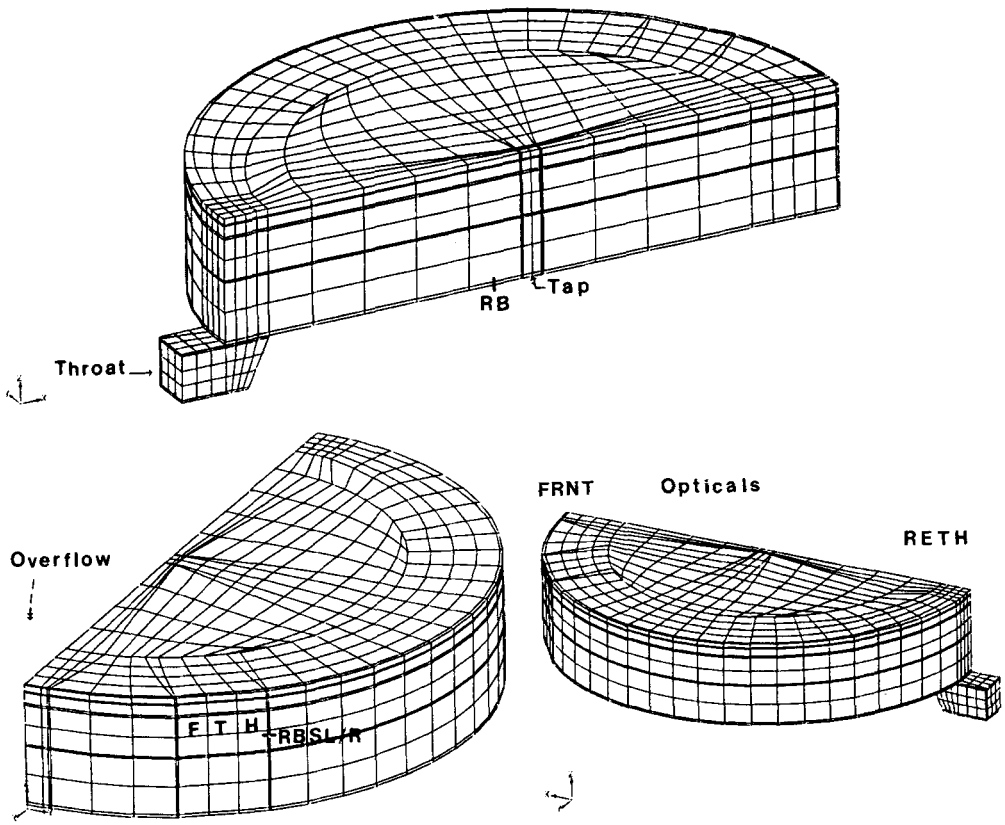

Figure 9. Television refiner mesh geometry: 1/2 of a circular TV refiner

The 3D analysis for the final Rayleigh number of order 10^6 showed that the temperature homogeneity at the forehearth connection was not affected by the radius and flow changes, nor were the surface velocities adversely affected. The recommendation to use the larger refiner was accepted and the system is presently being built.

PROCESS PROBLEM SOLVING—TUBING BOWL

A borosilicate tubing plant suffered through a period of inhomogeneous glass soon after start-up with a new cooling channel and bowl well. A quality improvement team was assigned to describe the sources of the problems and to propose operation changes which would reduce them to the target levels.

Part of the engineering team's work involved ascertaining what influence the forehearth and bowl well areas had on quality. Because of the complex contoured geometry of both the forehearth and the bowl well (Figure 13), a 3D FIDAP model was used to study the flow field of the glass as it moved downstream to the orifice. The majority of the cooling is done in the forehearth, with the bowl well serving to divert the glass around the shaft to set up the formation of the tubing at the orifice. By charting the various paths which glass could take and noting the stagnant regions in the channel and the obstruction effect of bowl shaft, specific quality problems oriented in a given

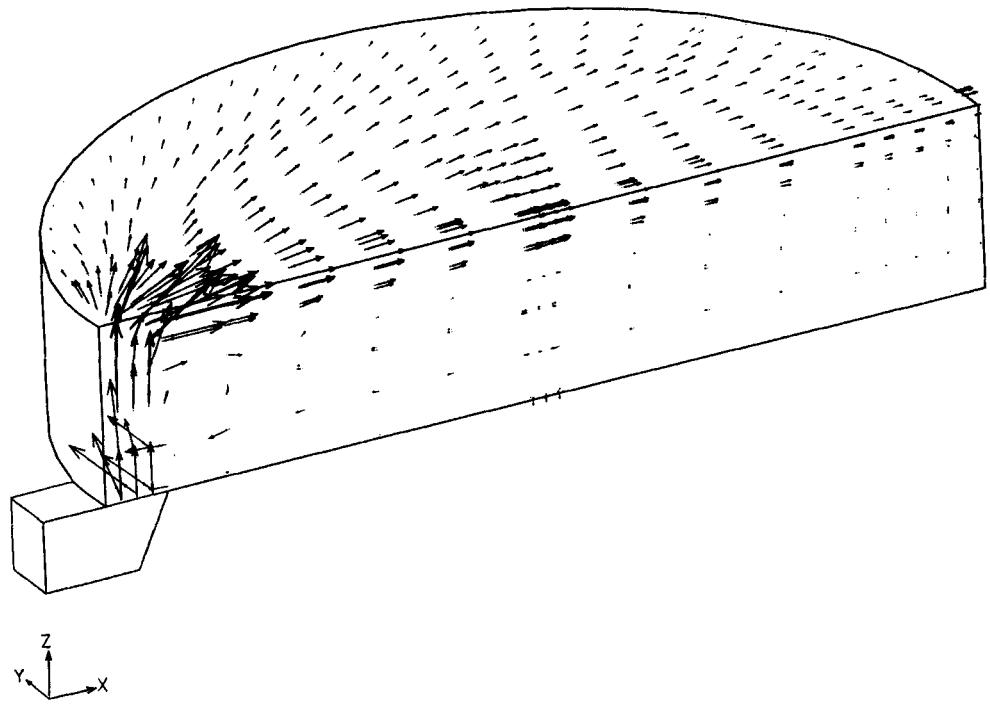

Figure 10. Television refiner $Ra = 10^4$ flow pattern: 1/2 of a circular TV refiner

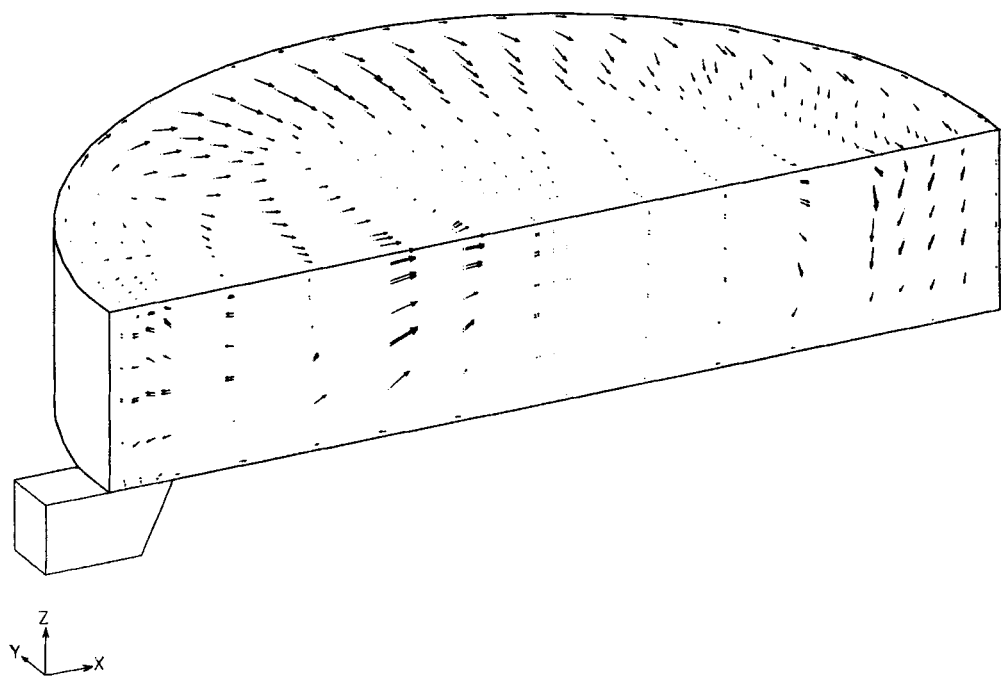

Figure 11. Television refiner flow at $Ra = 10^5$, three SS: 1/2 of a circular TV refiner

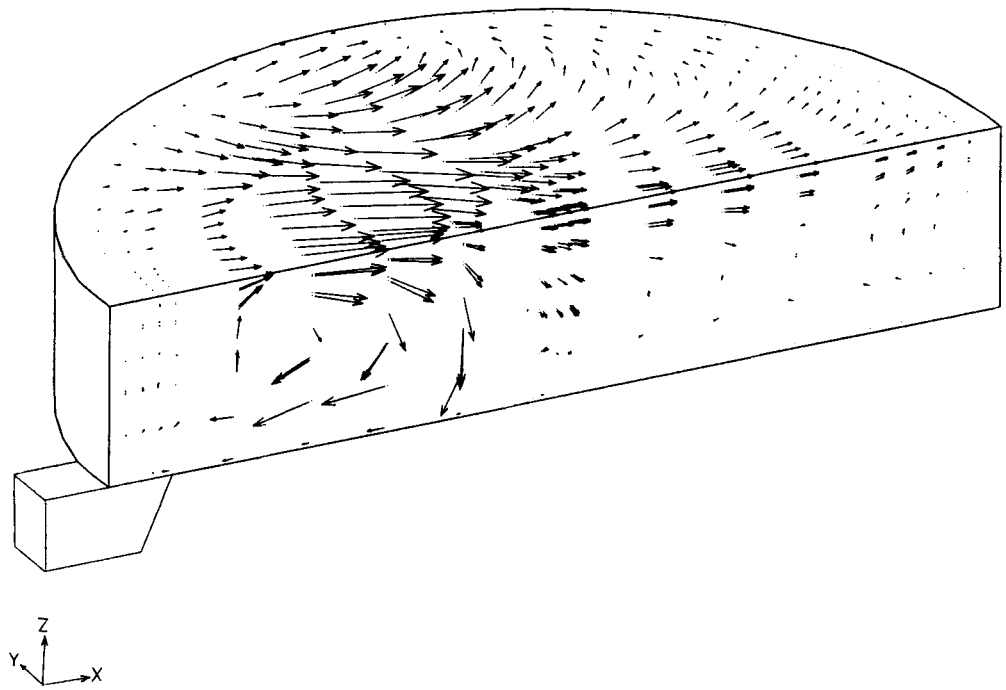

Figure 12. Television refiner flow at $Ra = 10^5$, six SS: 1/2 of a circular TV refiner

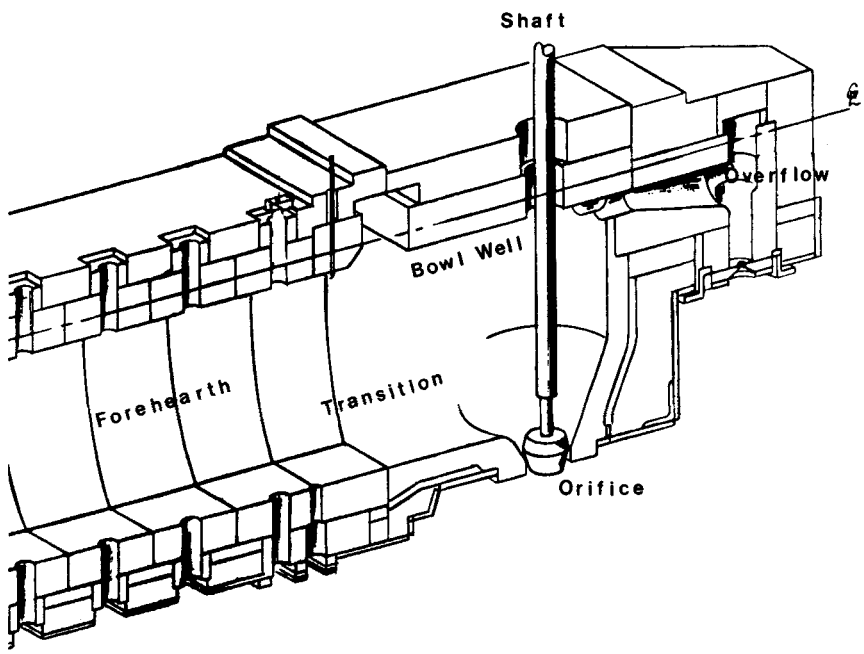

Figure 13. Tubing forehearth and bowl well physical design

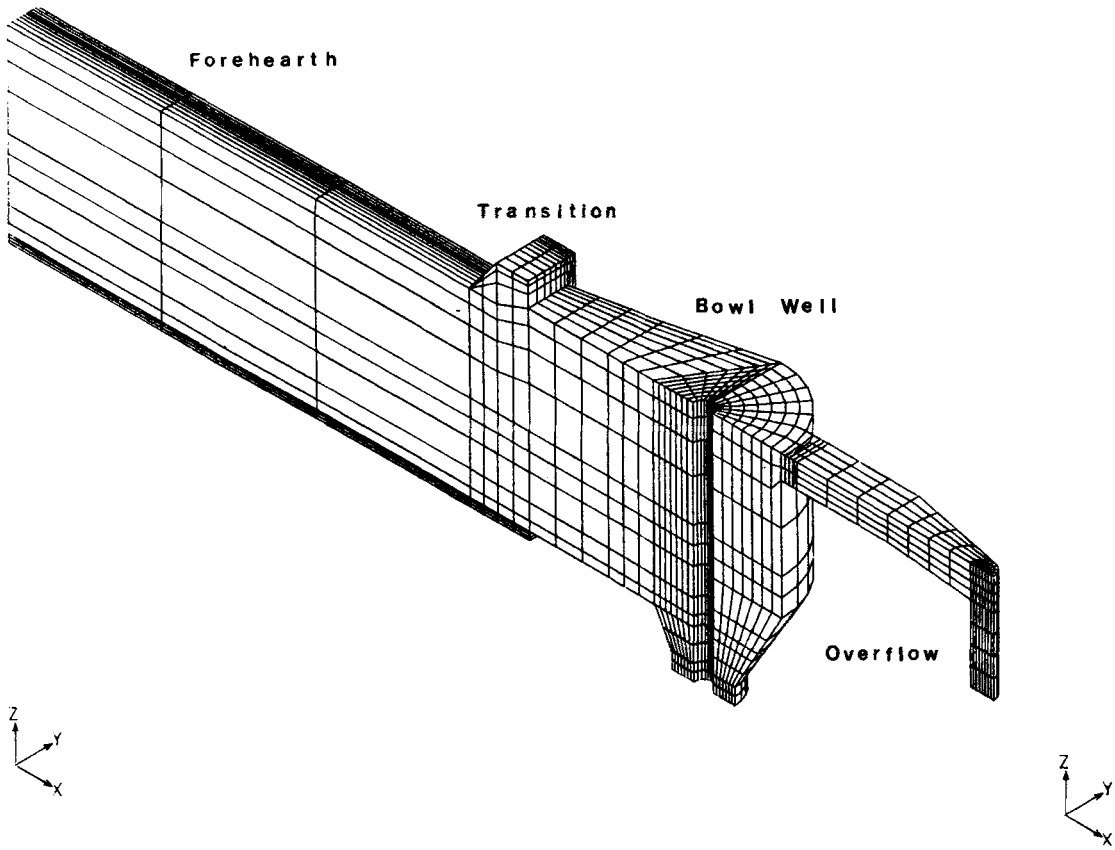

Figure 14. Tubing forehearth and bowl well mesh geometry: forehearth bowl well

tubing location could be mapped back to the source region. Knowing where the quality problem originated could be used to change the operation of the system in the area.

Tubing bowl mathematical model and numerical method

After careful consideration, the PDA/PATRAN-G software was chosen to create the mesh geometry. FIDAP's FIMESH program would have taken a longer development time to mesh the problem given its constraints to logic space and the absence of wedge and tetrahedral element generation. PATRAN provided an interactive capability in colour which was invaluable in constructing the forehearth and bowl well mesh. Since the model was assembled using 2D blueprints, PATRAN's ability to create automatically odd-shaped elements in the transition from a rectangular brick element to a cylindrical brick element was required. PATRAN also provided an easy method of zooming from a region described by a coarse number of nodes to a region with a finer mesh.

Figure 14 shows the mesh geometry of one half section of the forehearth and bowl assuming the flow is symmetric with respect to the centreline vertical plane. For future reference the section was divided into four regions: forehearth, transition zone, bowl well and overflow. The nodal points were concentrated around the transition and bowl well regions where the largest velocity and temperature gradients were anticiapted.

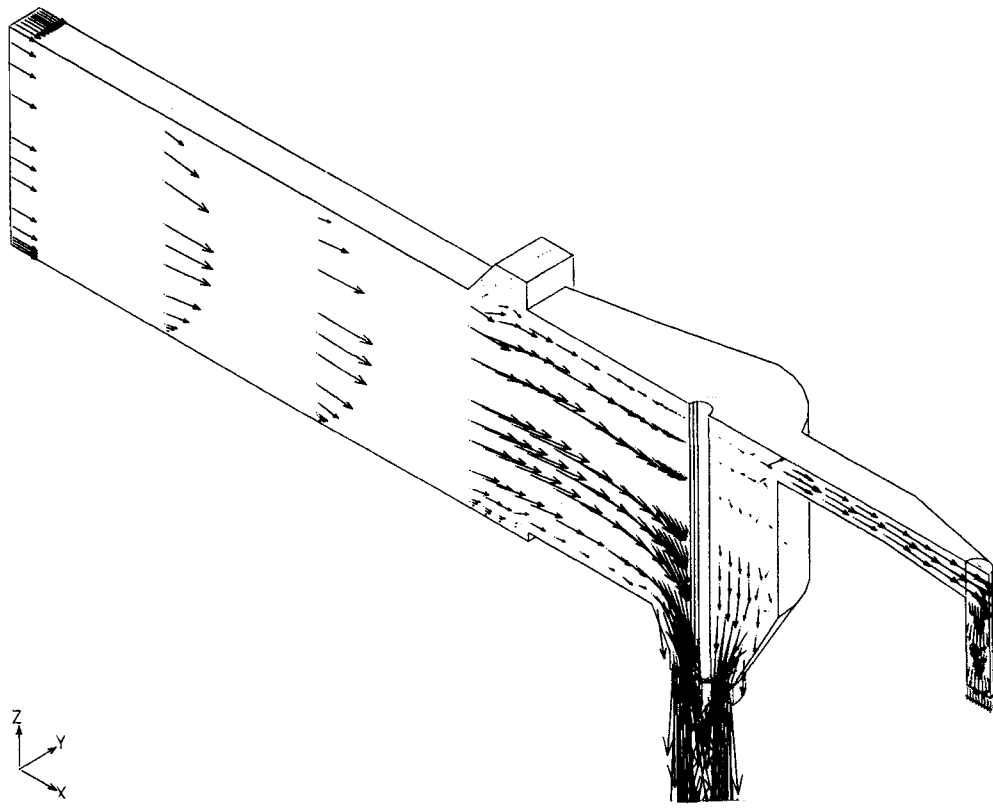

Figure 15. Tubing forehearth and bowl well velocities—centre plane view: forehearth and bowl well

Table V. Tubing bowl well problem size

Number of nodes	3841
Number of 3D elements	3718
Number of equations	10998
Number of matrix elements	11923194
Mean 1/2 bandwidth	542
Maximum 1/2 bandwidth	1193

The model was set up to duplicate an average operational condition when the process quality was unacceptable. The same mathematical formulation for glass flows used in the two previous examples was used to set up the problem. Following FDI's instructions, PATRAN's displacement constraint options were used to set the analogous FIDAP velocity and thermal boundary conditions. The inlet flow and temperature to the forehearth were specified, as well as the amount of glass exiting through the overflow. The refractory heat losses were imposed as heat transfer coefficients along the boundary. PATRAN created a neutral output file which was submitted to the PATRAN-to-FIDAP translator written by FDI to produce the FIPREP file.

Before submitting the job to FIDAP, several modifications were made. The FIPREP file was edited to add the control cards and the temperature-dependent physical properties of the

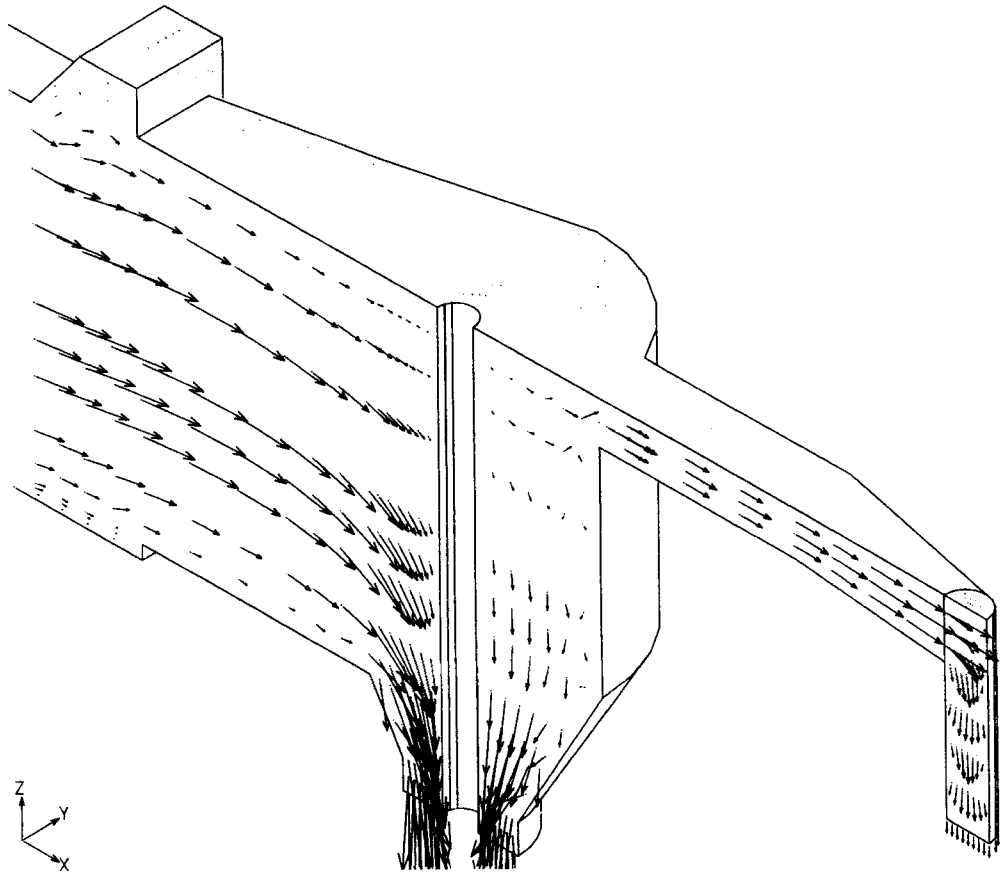

Figure 16. Bowl well velocities—zoom view along centre plane: forehearth and bowl well

borosilicate glass. Since the forehearth, bowl well and overflow temperatures were controlled with numerous electrical circuits, these were simulated in the model using FIDAP's subroutine for energy source terms.

The solution strategy used for this glass system reduced the variables to their dimensionless forms to minimize the effects of round-off error when using the penalty method. Since the glass viscosity is very high in this section of the process, both the Grashof and Reynolds numbers were much less than unity. At these levels no recirculating flow was anticipated and therefore the volumetric expansion coefficient 'stepping' scheme used in the previous cases was not needed. The problem was solved using the isothermal results as the initial field for the non-isothermal case which iterated through two SS and ten NR. Using the FPS 264 system, the solution time was 60 min. Table V contains information about the problem size for the tubing bowl case.

Tubing bowl well results and discussion

The 3D FIDAP simulation identified several interesting flow regimes. FIPOST was used extensively to view different flow planes within the bowl. Figure 15 shows the distribution of glass flow along the centreline vertical plane. As the glass passes through the transition zone into the

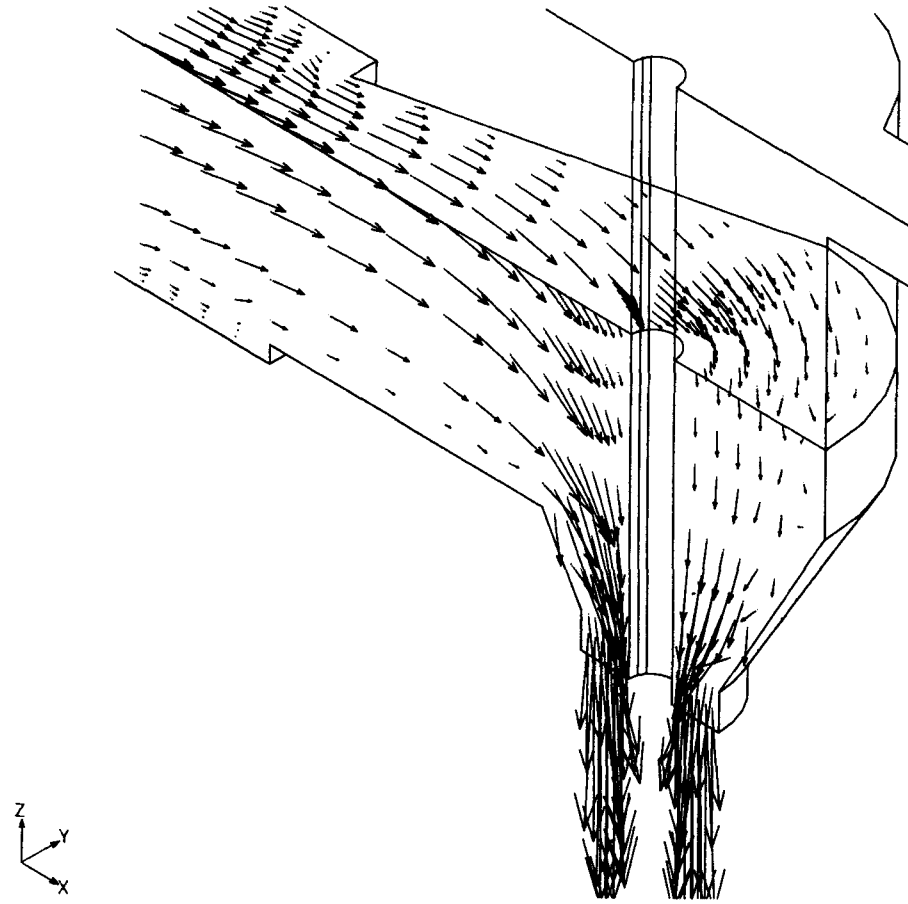

Figure 17. Transition zone and bowl well velocities—horizontal cut: forehearth and bowl well

bowl well it is forced to twist around the shaft in order to reach the orifice and overflow. The impedance of the shaft creates a geometric asymmetry in velocities at a given elevation around the shaft, with the upstream side moving faster than the downstream side (Figure 16). The region at the top of the shaft is inactive even though the overflow is positioned on the upper nose of the bowl well. Figure 17 shows a large stagnant region at the bottom entrance to the bowl well where the two different refractory flow cross-sections are connected. Downstream at the orifice the flow is very evenly distributed around the shaft.

A mapping study was performed on the flow from the forehearth to determine the final position of the glass particles in the tubing. Figure 18 shows several particle paths for glass on the centre plane (solid lines) and near the forehearth side (dotted lines) and the twisting effect of the bowl well. By relating the position of the quality defect in the tubing, the engineers can backtrack the path of the defect using the 3D model and isolate the upstream source.

CONCLUSIONS

The implementation of 3D finite element analyses for glass fluid flow and heat transfer problems has proven to be a cost-effective engineering tool for CGW. When compared with alternatives

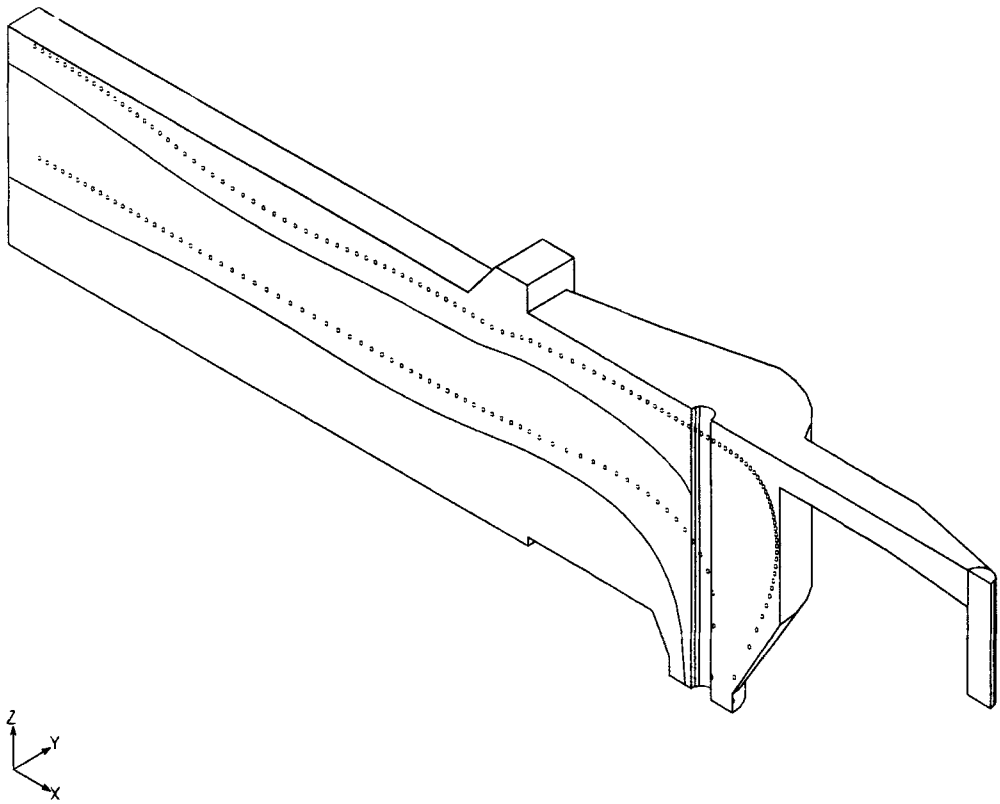

Figure 18. Tubing forehearth and bowl well particle paths: forehearth and bowl well

such as in-plant experimentation or small-scale laboratory testing, computer simulations offer a quicker and more flexible means to study the controlling process variables.

The investigations using FIDAP demonstrated the following:

1. An efficient mesh is important for the practical application of 3D finite elements to glass melters to insure convergence and numerical stability. 2D approximations can be used to determine suitable mesh patterns.
2. Mesh generation is easier with interactive software packages which take advantage of colour graphics and non-hexagonal element shapes. Wedge and tetrahedral elements are useful when minimizing the number of nodes while maintaining node refinement near the boundaries.
3. The high-Grashof-number and high-Prandtl-number flows seen in glass melters must be solved in loading steps using the buoyancy source term. There are a sufficient number of numerical methods to test various alternatives to determine the specific scheme for convergence.
4. Some program customization is needed to adapt to a glass melting process with electric power generation and to calculate energy balances.
5. The FIPOST post-processing program offers a useful qualitative way of interpreting the results of a problem. The ability to graphically display internal flow regimes makes explaining the results to production personnel much easier.

6. On the FPS 264 using the FMS library and attached to a VAX 780 host, the I/O is a large portion of the solution time.

REFERENCES

1. G. Leyens and J. Smrcek, 'Influence of tank depth and throughput on flow in glass tank furnaces', *Glastech. Ber.*, **55**(5), 81–87 (1982).
2. G. Leyens, 'Contribution to the calculation of two dimensional convection currents in continuous glass furnaces. Part 1. Mathematical model', *Glastech Ber.*, **47**(11), 251–259 (1974).
3. G. Hilbig, 'Problems in the three-dimensional mathematical modelling of electrically heated glass tank furnaces', *Glastech Ber.*, **57**(12), 301–306 (1984).
4. J. C. Carling, 'A reappraisal of the mathematical modelling of flow and heat transfer in glass tank forehearths', *Glass Technol.* **23**(5), 201–222 (1982).
5. M. S. Quigley and D. K. Kreid, 'Physical modeling of electric glass melting furnaces for high level waste immobilization', *ASME, Proc. 18th National Heat Transfer Conf.*, 2–15 August 1979.
6. D. A. Nolet, 'Applications of modeling and process analysis to furnace operations and redesign', *Proc. 46th Conf. on Glass Problems*, American Ceramic Society, 1986.
7. R. A. Murnane, 'Functional development of glassmelting process via modeling', *Ceram. Eng. Sci. Proc.*, **5**(1–2), 101–114 (1986).